

## **An Advanced Enrichment study of Gold Nanoparticles against the Bacterial Pathogen E.coli**

**Gargibala Satpathy<sup>1</sup> and E. Manikandan<sup>1,2</sup>**

<sup>1</sup>Central Research Laboratory/Department of Biotechnology, Sree Balaji Medical College and Hospital (SBMCH), Bharath Institute of Higher Education and Research, Chrompet, Chennai 600044, Tamil Nadu, India.

<sup>2</sup>Solid-State Nanoscale Laboratory, Dept. of Physics, TUCAS Campus, Thennangur-604408, Thiruvalluvar University, Vellore, India

### **Abstract**

Surface-enhanced Raman scattering (SERS) is a useful tool for label-free analysis of bacterial cell. In this current research, for study of sensitive, specific and reproducible Raman spectra, we optimized the methods and concentration of gold nanoparticles (AuNPs). To optimize the SERS enhancement method, the centrifugal force, method for preparing AgNPs, concentration of AuNPs, ionic strength of the solution used to suspend the cells and density of the cells were chosen as impact factors and optimized through orthogonal experiments. Finally, the improved method could generate sensitive and reproducible SERS spectra from single *Escherichia coli* cells, and the SERS signals primarily arose from the cell envelope.

### **Introduction**

Microorganisms belong to one of the biggest threats to humanity. The monitoring and detection of pathogenic and healthy bacteria are the keys to prevent and identify problems related to human health and safety [1,2]. Shiga toxin-producing *E. coli* (STEC), which comprise at least 100 serotypes, are considered as an important group of bacterial enter pathogens [3]. Rapid detection and identification of microbes in environmental, food and clinical samples is required for safety purposes as well as diagnosis of infectious diseases [4,5]. Conventional techniques for microbial detection, though reliable and gold standard, are time consuming, expensive and unsuitable for field situations [6,7]. Advent of novel techniques involving Nanotechnology has been promising for the development of rapid and low cost strategies for rapid detection and identification of microbes with higher sensitivity [8,9]. Gold nanoparticles find a significant place in medicine, material sciences as well as diagnostics for their unique optical and physiochemical properties [10,11]. The light absorption and emission characteristics of Gold Nanoparticles (GNPs) are exploited in detection and treatment of cancer [12,13]. The properties of Nanoparticles (NPs) give them high potential for use in various medical applications, particularly in diagnostics and therapy where they promise increased sensitivity, speed, and cost effectiveness. The Ultraviolet-

Visible and fluorescence properties of non-functionalized GNPs have not thus far been comprehensively documented. In view of the important features of SPR is analyzed with the combination of particles and nanostructures [14]. A notable plasmon provoked wonder is surface improved Raman scattering (SERS). The improved scattering found in SERS is a result of the electromagnetic and substance redesign [15]. This overhaul in the sign power makes this SERS procedure more effective and logical instrument with high sub-nuclear affectability and distinction is needed. The evident of huge number of fragments forming the bacterial cell such as starches, proteins, unsaturated fats. The (PEF) strategy is critical sign improvement is a direct result of two frameworks: excitation improvement and release improvement Point is to research antibacterial exercises of metal nanoparticles and their method of activity against pathogenic microbes on entire cell. We examine the biocidal properties of materials doped with metal and metalloid particles against the particular periodontal microorganisms were incorporated. The current examination ebb and flow research endeavors concerning the utilization of metal particles in periodontal infections treatment, while it calls attention to the difficulties and openings lying ahead. Here we report UV-Vis and antibacterial investigation AuNPs nanoparticles towards the methodology for identifying the pathogenic strain of *E.coli* cells. Point is to research antibacterial exercises of metal nanoparticles and their method of activity against pathogenic microbes on entire cell. Improvement properties of nanoparticles towards the bacterial cells.

### **Materials and Method**

New conditions of *Escherichia coli* pathogenic were gotten from (MTCC). Then *E.coli* was filtered into supplement stock which contains beaker for upcoming investigation. The Supplement stock solution is getting mixed withIn a thousand ml of water, dissolve 28 g of supplement agar. At 121<sup>0</sup> C, 15 lbs, for 30 minutes, the shaped solution plan was also carried out.

The expansion of the bacterial movement get settle in the single area of microorganism with a circle and vaccinating 25 ml of clean enhancement stock in a 100 ml cup. At the specific temperature of 37°C the carafe was replanting at 110 rpm over 24 hours. Afters the inoculum, 0.4 ml were shifted into an Erlenmeyer cup of 100 ml containing 25 ml improvement stock and agonised at 3-4 h at 37 °C and 100 rpm in a trembling incubation plant. One ml of a supplementary stock was then subsequently weakened to achieve an inferred target mixture of 1 x 10<sup>5</sup> units/ml (CFU, ml to 1) states. A lifestyle optical thickness at 660 nm assessed the number of species in the 4-hour culture. An optical thickness of some place in the scope of 0.1 and 0.3 was commonly identical to a gathering of between 10<sup>8</sup> CFU.ml<sup>-1</sup>. In the Raman spectrum which is highly recommended to work at room temperature, In this approach the a laser excitation is used to evaluate the at different specified size to amplifications, the outcomes are obtained at Excitation laser at 633 nm and granulating at 1200 lines/mm. The desire outcomes were stored in thermoelectrically cooled charge-coupled contraction locater. The given spectrum is obtained for 1 minute in its range at nominal temperature.

### **Results and conversations**

#### **Raman Microscopic Fingerprint Study**

In this analysis the relation among the pathogenic tissues and the NPs are more focused and the variations in the bacterial arrangements were mentioned and discussed with treated examples (Fig. 1.(a) and 1(b)) and (Fig.2(a) and 2(b)) show the standardized normal spectrum ranges without violating the specified limits of the test i.e from 500-1720  $\text{cm}^{-1}$ . The 2 extents of the spectrum is expressed in (Fig. 1a and 1b) and (Fig.2a and 2b). The main cell parts, including proteins, lipids, sugars and nuclear acids, have been identified. For eg, 547, 1000 and 1657  $\text{cm}^{-1}$  proteins [16], 1454  $\text{cm}^{-1}$  lipids were allocated to top of Raman proteins; Arredondo et al.2000), and nucleic acids (DNA/RNA) to the tops at 665, 778, and 1073  $\text{cm}^{-1}$  [17]. The Raman tops at 1046 and 1134  $\text{cm}^{-1}$  have been attributed primarily to starches [18,19], but there are also commitments from proteins and lipids [20]; Bianchi et al. There are several ambiguities in the literature regarding the role of vibrational unearthy microorganisms. Because of the unpredictability of microorganisms as a sub-atomic structure, it is unthinkable to presume to reliably relegate all Raman modes. The Raman spectra don't distinguish between pure atomic ordinary vibrations and the modes that emerge from various vibrational methods of particles that make up bacterial cells. The powers of explicit Raman modes assigned to sub-atomic vibrations associated with particular parts can be used to quantify these sub-atomic contrasts. In any case, when compared to their control part, ZnO-NPs show distinct differences, as seen in (Fig. 1) and (Fig. 2). (Fig.2). This striking difference may be due to the various cell segments present in these cells, as well as their unique communication instruments with ZnO-NPs. Progressions can be seen as Raman markers that are often combined with proteins, lipids, and DNA/RNA, as powers of a few pinnacles such as 1657, 1615, 1577, 1354, 1330, 1134, and 547  $\text{cm}^{-1}$ . Welcome data are provided by some pinnacle highlights (increase in Raman power), and boxes (decline in Raman strength).

Proteins constitute an enormous portion of the cell composition. The Raman spectrum in both *E. coli* strains is dominated by the vibration modes associated with proteins. The amide I vibration of proteins is a large Raman mode based on 1657  $\text{cm}^{-1}$  which is made of different basic partner units (such as  $\alpha$ -helix,  $\beta$ -sheets, self-defined circles, turning bits. As seen in Fig.1, an outstanding 1657  $\text{cm}^{-1}$  decrease in intensity suggests potential conformational changes in protein structures, such as the decrease in  $\alpha$ -helix Fig.2. Another wide band, approximately 547  $\text{cm}^{-1}$ , is devoted to disulfide bonds that is important for the identification of a tertiary protein structure. The decline in strength can be blamed on the impairment or nonetheless the breakage of disulfide bonds. Instead of these two modes, the Raman mode based on 1615  $\text{cm}^{-1}$  is highly susceptible to the micro-environment, which is sent to ring vibrations of sweet smelling amino acids (like tryptophan, tyrosine and phenylalanine). The presences of auxiliary proteins may result in increasing mode intensity because they affect the microenvironment of the amino corrosive deposits and cause hyperchromacity. Any of these advances is seen to have a significant degradation that can trigger the above-examined pinnacles to changes in their force and affect cell physiology.

### **Change in Lipids**

Lipids are the indispensable part of any cell divider that gives the cell fundamental trust. A crazy 1454  $\text{cm}^{-1}$  Raman lipid marker band, obvious in the Raman spectra of both the *E.coli*.

The CH curving methodologies for lipids are offered out to coli strains. Clearly, a jolting decline in power demonstrates conformational changes to the bilayer of the lipid, finally inciting hurt in the lipid structures. Additionally, such mischief prompts layer interference and unavoidably, prompts film break and cell spilling.

### Change in DNA/RNA

DNA and RNA, as well as a variety of nucleic acids, are the most fundamental components of cells. However, since their general amount is much smaller than proteins and lipids, the breakthrough characteristics of DNA and RNA in Raman go extremely small and are normally masked by the vibration of proteins and lipids. A Raman top based on the 1577  $\text{cm}^{-1}$  DNA and RNA band that is fully unprotected from the environment. DNA and RNA cannot be denatured by nucleobase unstock techniques and dRib tolerance of differentiating nucleosides due to insufficient denaturation, a phenomenal increase in the power of this mode is seen in the (Fig. 5.9) and (Fig. 5.10) efficiency expansion of this marker band. Furthermore, these denaturation and conformational changes result in hyperchromacity, which can influence the power decision of this mode. This is the result of the associated breakdown of DNA and RNA molecule fluctuations, which results in cell death.

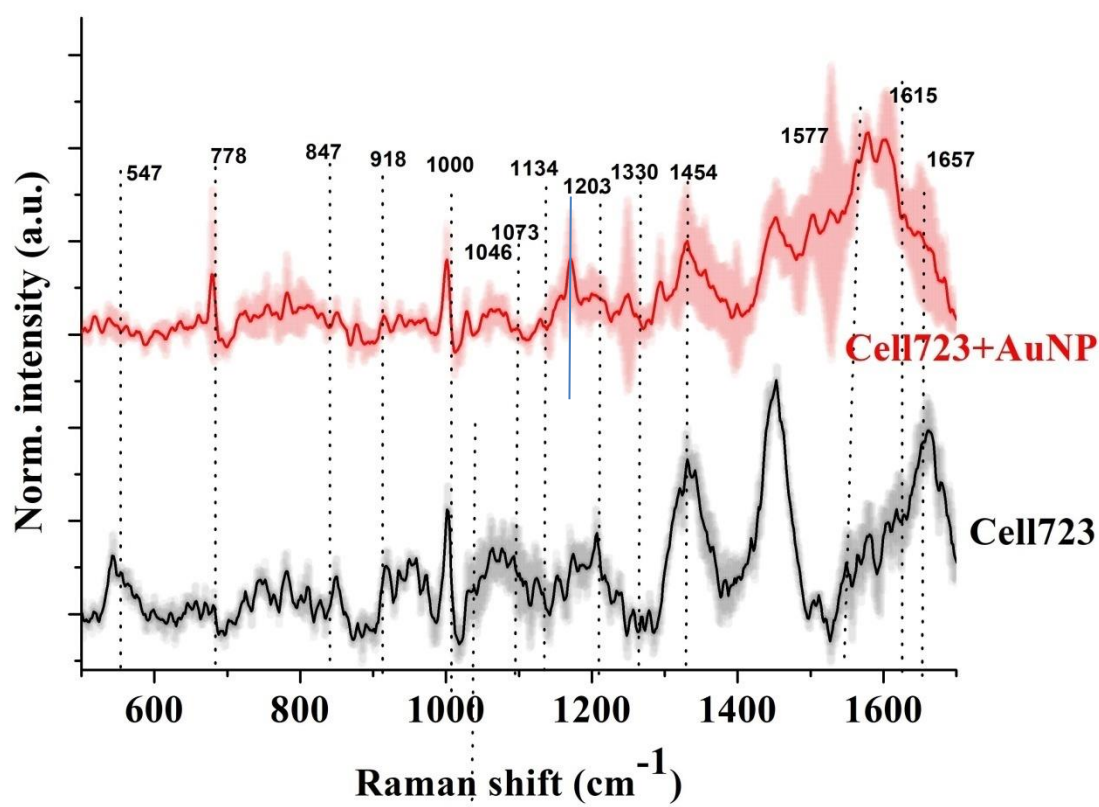
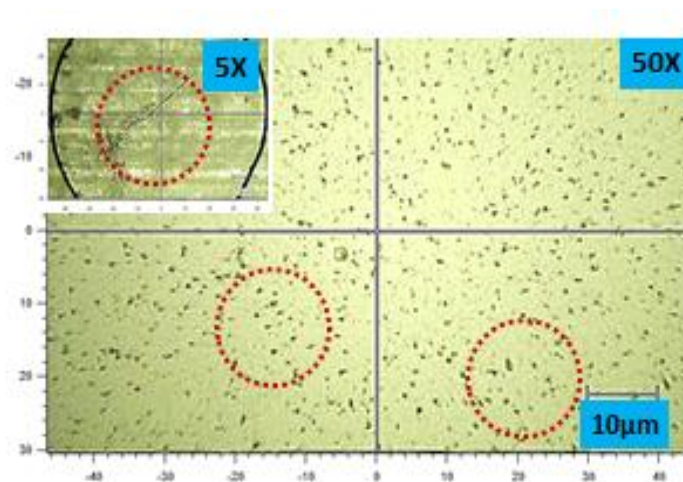
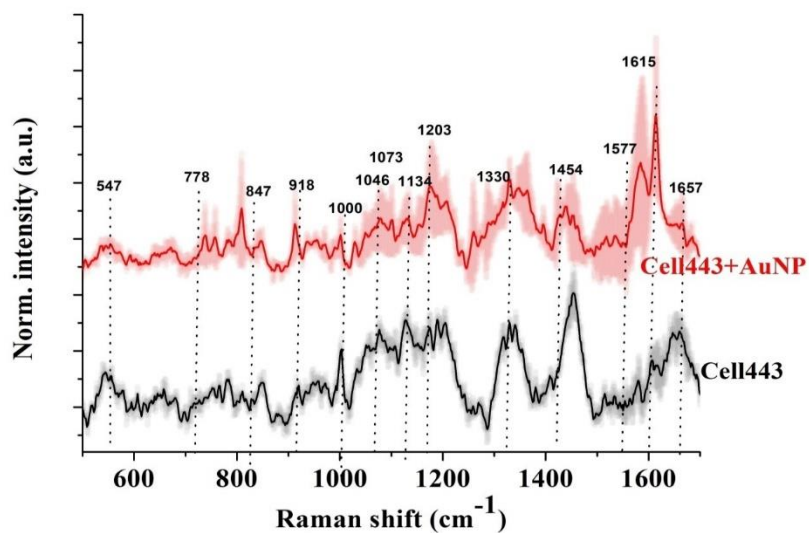


Fig.1:(a) Raman spectra of *E.coli* Strain MTCC723. Treated with  $10\text{mmol}^{-1}\text{Au-NPs}$ .



**Fig.1(b):**Raman microscopic image of *E.coli* Strain MTCC723. Treated with 10mmol<sup>-1</sup> Au-NPs



**Fig.2:(a)**Raman spectra of *E.coli* Strain MTCC443 treated with 10mmol<sup>-1</sup> Au-NPs

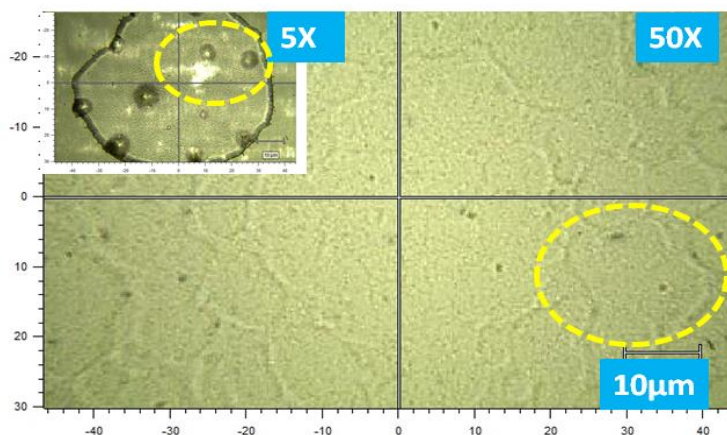


**Fig.2:(b)** Raman microscopic image of *E.coli* Strain MTCC443 treated with 10mmol<sup>-1</sup> Au-NPs

## Final thoughts

We prefer to use non-destructive visible lighting and Raman small qualitative testing methods in this experimental study to shoot the most recent developments, implementations and future patterns in microorganism detection. The Raman distinction spectra clearly show the forceful amendment of Raman marker bands of proteins and lipids as opposed to DNA/RNA bands. The SPR property of Au-NPs resulted in increased visible light for each pathogen. Raman analysis and part study revealed significant differences in the interaction of the two strains with Au-NPs thanks to macromolecule, super molecule, and DNA/RNA evoked conformational changes.

## References

1. Proceedings of the 4th IPLeiria's International Health Congress: Leiria, Portugal. 11-12 May 2018. (2018). *BMC Health Services Research*, 18(Suppl 2), 684. <https://doi.org/10.1186/s12913-018-3444-8>
2. Mogrovejo, D. C., Perini, L., Gostinčar, C., Sepčić, K., Turk, M., Ambrožič-Avguštin, J., Brill, F., & Gunde-Cimerman, N. (2020). Prevalence of Antimicrobial Resistance and Hemolytic Phenotypes in Culturable Arctic Bacteria. *Frontiers in microbiology*, 11, 570. <https://doi.org/10.3389/fmicb.2020.00570>
3. Gajdács M. (2019). The Continuing Threat of Methicillin-Resistant *Staphylococcus aureus*. *Antibiotics (Basel, Switzerland)*, 8(2), 52. <https://doi.org/10.3390/antibiotics8020052>
4. Romano, S., Jackson, S. A., Patry, S., & Dobson, A. (2018). Extending the "One Strain Many Compounds" (OSMAC) Principle to Marine Microorganisms. *Marine drugs*, 16(7), 244. <https://doi.org/10.3390/md16070244>
5. Mogrovejo, D. C., Perini, L., Gostinčar, C., Sepčić, K., Turk, M., Ambrožič-Avguštin, J., Brill, F., & Gunde-Cimerman, N. (2020). Prevalence of Antimicrobial Resistance and Hemolytic Phenotypes in Culturable Arctic Bacteria. *Frontiers in microbiology*, 11, 570. <https://doi.org/10.3389/fmicb.2020.00570>
6. Mehete, G. T., Leo, V. V., Singh, G., Sorokan, A., Maksimov, I., Yadav, M. K., Upadhyaya, K., Hashem, A., Alsaleh, A. N., Dawoud, T. M., Almaary, K. S., & Singh, B. P. (2021). Current Developments and Challenges in Plant Viral Diagnostics: A Systematic Review. *Viruses*, 13(3), 412. <https://doi.org/10.3390/v13030412>
7. Basha, I., Ho, E., Yousuff, C. M., & Hamid, N. (2017). Towards Multiplex Molecular Diagnosis-A Review of Microfluidic Genomics Technologies. *Micromachines*, 8(9), 266. <https://doi.org/10.3390/mi8090266>
8. Shafiq, M., Anjum, S., Hano, C., Anjum, I., & Abbasi, B. H. (2020). An Overview of the Applications of Nanomaterials and Nanodevices in the Food Industry. *Foods (Basel, Switzerland)*, 9(2), 148. <https://doi.org/10.3390/foods9020148>
9. Sharma, A., Mishra, R. K., Goud, K. Y., Mohamed, M. A., Kummari, S., Tiwari, S., Li, Z., Narayan, R., Stanciu, L. A., & Marty, J. L. (2021). Optical Biosensors for Diagnostics of Infectious Viral Disease: A Recent Update. *Diagnostics (Basel, Switzerland)*, 11(11), 2083. <https://doi.org/10.3390/diagnostics11112083>
10. Amina, S. J., & Guo, B. (2020). A Review on the Synthesis and Functionalization of Gold Nanoparticles as a Drug Delivery Vehicle. *International journal of nanomedicine*, 15, 9823–9857. <https://doi.org/10.2147/IJN.S279094>
11. Bharadwaj, K. K., Rabha, B., Pati, S., Sarkar, T., Choudhury, B. K., Barman, A., Bhattacharjya, D., Srivastava, A., Baishya, D., Edinur, H. A., Abdul Kari, Z., & Mohd Noor, N. H. (2021). Green Synthesis of Gold Nanoparticles Using Plant Extracts as Beneficial Prospect for Cancer Theranostics. *Molecules (Basel, Switzerland)*, 26(21), 6389. <https://doi.org/10.3390/molecules26216389>
12. Silva, C. O., Petersen, S. B., Reis, C. P., Rijo, P., Molpeceres, J., Fernandes, A. S., Gonçalves, O., Gomes, A. C., Correia, I., Vorum, H., & Neves-Petersen, M. T. (2016). EGF Functionalized Polymer-Coated Gold Nanoparticles Promote EGF Photostability and EGFR Internalization for Photothermal Therapy. *PLoS one*, 11(10), e0165419. <https://doi.org/10.1371/journal.pone.0165419>

13. Xia, Y., Chen, H., Zhang, F., Bao, C., Weir, M. D., Reynolds, M. A., Ma, J., Gu, N., & Xu, H. (2018). Gold nanoparticles in injectable calcium phosphate cement enhance osteogenic differentiation of human dental pulp stem cells. *Nanomedicine : nanotechnology, biology, and medicine*, *14*(1), 35–45. <https://doi.org/10.1016/j.nano.2017.08.014>
14. Prabowo, B. A., Purwidyantri, A., & Liu, K. C. (2018). Surface Plasmon Resonance Optical Sensor: A Review on Light Source Technology. *Biosensors*, *8*(3), 80. <https://doi.org/10.3390/bios8030080>
15. Wang, D., Loo, J., Chen, J., Yam, Y., Chen, S. C., He, H., Kong, S. K., & Ho, H. P. (2019). Recent Advances in Surface Plasmon Resonance Imaging Sensors. *Sensors (Basel, Switzerland)*, *19*(6), 1266. <https://doi.org/10.3390/s19061266>
16. Zolotareno, A., Chekalin, E., Mesentsev, A., Kiseleva, L., Gribanova, E., Mehta, R., Baranova, A., Tatarinova, T. V., Piruzian, E. S., & Bruskin, S. (2016). Integrated computational approach to the analysis of RNA-seq data reveals new transcriptional regulators of psoriasis. *Experimental & molecular medicine*, *48*(11), e268. <https://doi.org/10.1038/emm.2016.97>
17. Resnik-Docampo, M., & de Celis, J. F. (2011). MAP4K3 is a component of the TORC1 signalling complex that modulates cell growth and viability in *Drosophila melanogaster*. *PloS one*, *6*(1), e14528. <https://doi.org/10.1371/journal.pone.0014528>
18. Rodríguez-Durán, L. V., Valdivia-Urdiales, B., Contreras-Esquivel, J. C., Rodríguez-Herrera, R., & Aguilar, C. N. (2011). Novel strategies for upstream and downstream processing of tannin acyl hydrolase. *Enzyme research*, *2011*, 823619. <https://doi.org/10.4061/2011/823619>
19. Serebrennikova, K. V., Berlina, A. N., Sotnikov, D. V., Zherdev, A. V., & Dzantiev, B. B. (2021). Raman Scattering-Based Biosensing: New Prospects and Opportunities. *Biosensors*, *11*(12), 512. <https://doi.org/10.3390/bios11120512>
20. Gómez Castaño, J. A., Boussekey, L., Verwaerde, J. P., Moreau, M., & Tobón, Y. A. (2019). Enhancing Double-Beam Laser Tweezers Raman Spectroscopy (LTRS) for the Photochemical Study of Individual Airborne Microdroplets. *Molecules (Basel, Switzerland)*, *24*(18), 3325. <https://doi.org/10.3390/molecules24183325>